PCCP

Accepted Manuscript

ROYAL SOCIETY OF CHEMISTRY

www.rsc.org/pccp

Physical Chemistry Chemical Physics
CREATED USING THE RSC LaTeX PCCP ARTICLE TEMPLATE – SEE www.rsc.org/electronicfiles FOR DETAILS
ARTICLE TYPE www. rsc.org/xxxxxx | XXXXXXXX

Theory of non-equilibrium critical phenomena in three-dimensional condensed systems of charged mobile nanoparticles

V.N. Kuzovkov,*[a] G. Zvejnieks,[a] and E.A. Kotomin[b]

Received Xth XXXXXXXXXX 20XX, Accepted Xth XXXXXXXXX 20XX
First published on the web Xth XXXXXXXXXX 200X
DOI: 10.1039/b000000x

A study of 3d electrostatic self-assembly (SA) in systems of charged nanoparticles (NP) is one of the most difficult theoretical problems. In particular, the limiting case of negligible or very low polar media (e.g. salt) concentration, where the long-range NPs interactions cannot be reduced to commonly used effective short-range (Yukawa) potentials, remains unstudied. Moreover, the present study has demonstrated that unlike the Debye-Hückel theory, a complete screening of the charges in SA kinetics (dynamic SA) is not always possible. Generally speaking, one has to take into account implicitly how each NP interacts with all other NPs (the true long-range interactions). Traditional theoretical methods allow us to monitor such the electrostatic 3d system kinetics only at very short times, which is far from sufficient for the understanding the dynamic SA. In this paper, combining an integrated analytical approach (nonlinear integro-differential kinetic equation for correlation functions) and reverse Monte Carlo in 3d case, we have obtained the self-consistent solution of this challenging problem. We demonstrate, in particular, the existence of critical points and critical phenomena in the non-equilibrium kinetics in a 3d system of oppositely charged mobile NPs.

1 Introduction

In the last decades nanoparticles (NPs) of different materials (metals, semiconductors, oxides) have been successfully synthesized and functionalized with charged ligands [1]. These NPs could be used in nanoscale *self-assembly* (SA) as building blocks in fabrication of ordered functional structures with representative applications [2,3]. The SA studies in solutions containing mobile and oppositely charged NPs (electrostatic SA) are very important due to numerous manifestations of this phenomenon in crystals, polymers, nano-, bio-molecules or aggregates [4,5]. In the electrostatic SA the competition between long-range (electrostatic) and short-range (van der Waals) interactions plays a very important role [6–10].

Note that without the electrostatic interaction the NPs only attract each other, which greatly limits the variety of options for SA manifestation. At the same time, the electrostatic interactions can be both attractive and repulsive, the interaction potential and its effective radius could vary due to several reasons, including the change in the dielectric constant of polar medium or concentration of ions present in solution. The study of NPs SA could give a solid basis for understanding more complex biological systems [11–13]. Here, an important step is to study the interactions between charged NPs and biological macromolecules [1,14]. From a theoretical point of view, the description of biomolecular systems and description of NPs could be performed within a general approach based on the coarse-grained models [15]. So, for both systems, attention is paid only to the essential features of the problem, while less important details are described via average quantities. We believe that the fundamental laws discussed in this paper governing the behavior of systems with electrostatic interaction have a scope, far beyond the specific subject of NPs.

The dynamic (kinetic) aspects of SA formation are of a fundamental importance. The typical equilibration time for many real systems could take hours or days, within this period the system remains far from equilibrium. Moreover, as is well known, non-equilibrium structures (dynamic SA, DySA [16,17]) often differ strongly from those at equilibrium. The realistic study of the 3d DySA with charged mobile NPs imposes very strict requirements on theory.

Note some problems arising in the study of condensed systems with long-range (electrostatic) interactions [1]. For oppositely charged NPs in polar solutions the salt effect is very important: inorganic salts determine the assembly of charged NPs into different composite structures because the magnitudes of electrostatic interactions are defined, in particular, by salt concentrations. For example, for negligible or low salt concentrations, the charged NPs nucleate and grow into all-NP crystals, but at higher salt concentrations the NPs start to form supraspheres [4] because varying the salt concentration could change dramatically the many-particle screening effects. Note also that these effects cannot be described by introducing only one time-independent parameter - the Debye screening length r_D. The chemical nature of salts is also important:

[a] *Institute for Solid State Physics, University of Latvia, Riga, Latvia. E-mail: kuzovkov@latnet.lv*
[b] *Max-Planck Institute for Solid State Research, Stuttgart, Germany*

for the same Debye screening length r_D different salts could induce formation of quite different ordered structures[4].

The 3d case of negligible or low salt concentrations lies beyond ability of the traditional theoretical methods (Molecular Dynamics and Kinetic Monte Carlo (KMC)) because here one has to consider explicitly the contribution of the long-range interactions of a given NP with all other NPs, which is computationally hardly possible. For this reason, almost all simulations of 3d systems were carried out so far in the limit at *high salt concentrations* (strong Coulomb screening), when exact long-range Coulomb potentials have been replaced by the effective short-range Yukawa ones[18,19]. However, there are limitations even within this approximation. Typical simulations[18] show that after the initial stage of a very rapid formation of small aggregates, further SA processes becomes very slow. Thus, the formation of larger clusters or ordering at intermediate and long length scales requires very long times. There exist practically no computational methods able to monitor the evolution of 3d ionic systems for such long simulation times. For these practical reasons, nowadays the study of electrostatic DySA is limited primarily to 2d systems[6,7].

In the present paper, we demonstrate a significant progress in this important modeling area. Our new approach is based on a fundamental change in the method for SA kinetics study. Instead of stochastic modeling of systems with a small number of particles (which is small for statistics, but still large for the calculation of the all interaction energies between particles), we use the *combined* method[8–10]. This method is primarily based on the numerical solution of the (integro-differential) kinetic equations for the pair correlation functions, which in fact coincide with the *radial distribution functions* known in statistical physics of equilibrium systems. From these distribution functions after special transformations the system's structural information (partial structure factors, screening factors, typical snapshots of the structure) are derived. The main idea of this approach was formulated not long ago[8], but so far was practically implemented only for 2d systems[9,10], including systems with chemical reactions[20].

In this paper, using a new method we revisit DySA systems with mobile and charged NPs[8–10] in the limiting case of negligible salt concentrations (absence of salt, weak charge screening), for which no results were obtained so far. For the first time we are able to study SA kinetics in 3d systems. Another limiting case (intermediate and high salt concentrations) will be considered in our next paper. In this paper we have studied the behavior of long-wavelength fluctuations of the particle densities in systems with electrostatic SA and demonstrated a deep analogy between the equilibrium critical phenomena and the electrostatic SA for systems far from equilibrium. The results of this study may be important, in particular, for understanding the formation mechanism of internally connected SA nanostructures in ionic liquids[21,22].

2 Model and parameters

We generalize the model previously studied in 2d case, Refs.[6–10], for 3d. To simulate the short-range van der Waals (dispersion) interactions between oppositely charged A and B particles (molecules), the classical 6-12 Lennard-Jones potential is used

$$U(r) = 4U_0[(\frac{r_0}{r})^{12} - (\frac{r_0}{r})^6]. \quad (1)$$

We minimize a number of free parameters by assuming U_0 and r_0 are the same for similar (AA, BB) and dissimilar (AB) pairs. The Lennard-Jones potential corresponds to the particle repulsion as short distances, $r < r_c = 2^{1/6} r_0$ (due to finite particle sizes) and attraction at larger distances, $r > r_c$. We assume similar repulsion of both similar and dissimilar pairs of NPs at $r < r_c$ but cut the dissimilar pair attraction at $r > r_c$[6,8,23]. In other words,

$$U_{AA}(r) = U_{BB}(r) = 4U_0[(\frac{r_0}{r})^{12} - (\frac{r_0}{r})^6], \quad (2)$$

and

$$U_{AB}(r) = 4U_0[(\frac{r_0}{r})^{12} - (\frac{r_0}{r})^6 + \frac{1}{4}] \quad (3)$$

for $r \le r_c = 2^{1/6} r_0$, and $U_{AB}(r) \equiv 0$ for $r > r_c$ (truncated and shifted Lennard-Jones potential[23]). It means that without Coulomb interactions dissimilar NPs, A and B, repel each other whereas similar NPs (A-A, B-B) attract each other and thus could aggregate. It is convenient to use dimensionless temperature parameter $\theta = k_B T / U_0$.

The long-range Coulomb interactions have the standard form ($\alpha, \beta = A, B$):

$$U^C_{\alpha\beta}(r) = \frac{e_\alpha e_\beta}{\varepsilon r}, \quad (4)$$

where ε is the dielectric constant and e_A and e_B particle charges. We consider here the limiting case without polar media (salt). In this case there are no (small) ions except NPs in the system. Therefore, screening of long-range potential, if any, is the result of the spatial redistribution of charged NPs.

The NPs are assumed to have opposite charges Z: $e_A = Z_A e$, $e_B = -Z_B e$ (the value of $Z_B = 1$ is fixed) and an effective diameter r_0, NPs densities are n_A and n_B. The principle of electroneutrality leads to $Z_A n_A = Z_B n_B$. The Coulomb potential is described by a single dimensionless parameter $\zeta = l_B / r_0$, where l_B is the Bjerrum length,

$$\zeta = \frac{e^2}{\varepsilon k_B T r_0}. \quad (5)$$

The length unit r_0 and the diffusion time unit $t_0 = r_0^2/(D_A + D_B)$ are used hereafter. Additionally, the total particle density (concentration), $n = n_A + n_B$, determines the dimensionless parameter $\eta = n r_0^3$, whereas asymmetry in the particles' diffusion coefficients is described by the parameter $\mu =$

$D_A/(D_A+D_B)$. In the following a definition of the structure factors will be introduced dependent on the wave number q. Accordingly, it is taken in the unit of r_0^{-1}.

3 Methods

3.1 Smoluchowski-type equations

The complete set of kinetic equations[8] is of Smoluchowski-type:

$$\frac{\partial F_{\alpha\beta}(r,t)}{\partial t} = D_{\alpha\beta}\nabla[\nabla F_{\alpha\beta}(r,t) + \frac{F_{\alpha\beta}(r,t)}{k_BT}\nabla W_{\alpha\beta}(r,t)], \quad (6)$$

where $D_{\alpha\beta} = D_\alpha + D_\beta$ is the coefficient of mutual diffusion. We do not discuss in detail derivation of the equation set since it was done in detail in Ref.[8]. We note only that they coincide with the first *exact* equations based on many-body theory (very similar to the Bogolyubov - Born - Green - Kirkwood - Yvon (BBGKY) hierarchy, see also Ref.[24,25]). The eq. (6) for the complete set of joint correlation functions, $F_{\alpha\beta}(r,t)$, describes the effective particle diffusion in potentials of mean forces, $W_{\alpha\beta}(r,t)$, that are, in its turn, functionals of the correlation functions $F_{\alpha\beta}(r,t)$ (self-consistent theory). In the two-component (A,B) systems under consideration three *time-dependent* functions are used: two for similar particles, $F_{AA}(r,t)$ and $F_{BB}(r,t)$, and one for dissimilar, $F_{AB}(r,t)$. The set of coupled kinetic non-linear and integro-differential equations (6) is solved numerically by using standard methods of discretization and a recurrent procedure for non-linear terms[8].

Note that the *form* of first equations (6) is exact whereas the effective potentials of mean forces, $W_{\alpha\beta}(r,t)$, are obtained *approximately*. Two main approximations are used here: (i) The electrostatic contribution to the potentials of mean forces is found by a solution of Poisson equation (a self-consistent solution): we are looking for the electrostatic potential $\phi(r,t)$ produced by a spatial distribution of charged particles (which, in turn, depends on the potential):

$$\nabla^2\phi(r,t) = -\frac{4\pi}{\varepsilon}\rho[F(r,t)]. \quad (7)$$

The charge density ρ can be easily related to the densities of NPs and the joint correlation functions[8], $\rho = \rho[F(r,t)]$. (ii) The second, so-called Kirkwood approximation[26] is used for contribution of short-range interactions in the potentials of mean forces[8]. Its use in the kinetic problems described by Smoluchowski-type equations, and evaluation of its accuracy is discussed in detail in Ref.[24,25].

3.2 Joint correlation functions

The statistical meaning of the joint correlation functions is fully analogous to the radial distribution function in statistical physics of dense gases and liquids: the quantities

$$C_\beta^{(\alpha)}(r,t) = n_\beta F_{\alpha\beta}(r,t) \quad (8)$$

are average densities of NPs β-type at the relative distance r provided that a probe particle α is placed into the coordinate origin[24] and n_β are macroscopic densities of β-type NPs. If one knows the average particle densities, eq.(8), the average charge densities entering eq.(7) could be simply found[8]. The joint correlation functions are normalized to unity (no spatial correlations, random distribution of particles at long distances)

$$F_{\alpha\beta}(\infty,t) \equiv 1. \quad (9)$$

The deviation of the correlation function above the unity means local concentration surplus of NPs, below unity - depletion with respect to the random distribution.

We consider here the ordering formation process from chaos: random initial distribution of NPs is used, $F_{\alpha\beta}(r,0) = 1$, which corresponds to a well stirred system and commonly used in self-organization studies.

3.3 Transformation of information

It is well known that the correlation functions $F_{\alpha\beta}(r,t)$ are of fundamental importance because they determine all macroscopic thermodynamic quantities (compressibility, average internal energy per particle, etc.). However, the information contained in the correlation functions is fairly abstract. First of all, the correlation function does not describe the distribution of the particles in a real space, this is only a distance-dependent distribution of *particle pairs*.

Fig.1 shows four examples of different distributions of particles described by the correlation functions. Using definitions, eq.(8) one can determine the location of the particles in the nearest coordination spheres around the particle placed in the coordinate center. However, to estimate the location of the particle at larger distances from the center is almost impossible. The reason is trivial, this information is contained in the small deviations of the correlation functions from their asymptotic behavior, eq.(9).

In the analysis of pattern formation in systems with electrostatic SA, it is important to analyze the large-scale fluctuations of the particle densities. This information can be obtained by using the so-called *partial structure factors* $S_{\alpha\beta}(q,t)$, at small values of wave number q. In this paper the Faber-Ziman[27] definition is used

$$S_{\alpha\beta}(q,t) = 1 + n\int_0^\infty [F_{\alpha\beta}(r,t) - 1]\frac{\sin(qr)}{qr}4\pi r^2 dr. \quad (10)$$

Note that both methods - use of the correlation functions $F_{\alpha\beta}(r,t)$ or the structural factors $S_{\alpha\beta}(q,t)$ - have one common drawback: they are abstract. Indeed, it is essential to get

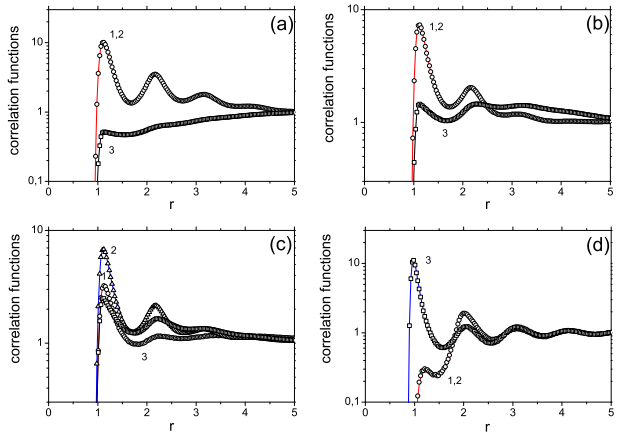

Fig. 1 (Color online) Quality of the 3d RMC method: (a) the joint correlation functions (curves (1) AA, (2) BB, and (3) AB pairs) obtained from kinetic equations (line) and RMC (symbols) for snapshots in Fig.3a,c; (b) shows the same functions for snapshots in Fig.5b,d; (c) for snapshots Fig.8b,d; (d) for snapshots in Fig.10b,d.

spatial 3d images of arising structures and their components (typically clusters in liquids, their size distribution, etc.).

We discussed in recent Refs.[8,28] new ideas of the so-called Reverse MC (RMC) method that is based on the goodness-of-fit statistical model, e.g. the Pearson χ^2 test correlation functions. This method is used here to visualize pattern formation in 3d. Previous ideas[8] were developed for 2d systems and had certain limitations of the accuracy. Note also that the very idea of the RMC method is not new (see, for example, Refs.[29,30]), but it has been previously used mainly for the treatment of experimental data on the structural factors of the system. The latter was determined, however, not in the whole range of wave numbers q, and functions were not smooth due to experimental errors.

An advantage of the RMC is that it is independent on specific interparticle interactions. The problem is reduced to achieving the best possible coincidence between set of the correlation functions obtained by numerical solution of eqs.(6) (called the *test functions*) and another set of correlation functions, obtained by means of the Monte Carlo method. The latter distribution of particles is modeled by randomly selecting a particle and generating its new spatial coordinates. One calculates a function (goodness-of-fit for statistical model) controlling the convergence of the method. As can be seen from Fig.1 with both sets of correlation functions - solutions of kinetic equations (lines) and the RMC (symbols) - in principle, it is possible to match both sets of correlation functions with any desirable degree of accuracy (for liquid-like disordered structures[28]). As a result, we map the information from the correlation functions into the distribution of particles in the real 3d space in the form of characteristic snapshots. Moreover, as shown in Ref.[28], it is possible to find not only a series of complete snapshots of the structure, but also to explore its details, such as the distribution of aggregates (clusters) in size, or to find the maximum size or a typical cluster. In the case of liquid systems, this information has a well-istablished statistical characteristics. In contrast to discrete case, the continuous case requires a definition of nearest neighboring (NN). Here we define NN as particles which are separated closer than $r_c = 2^{1/6} r_0$.

Note that by solving the Poisson eq.(7) in spherical coordinates, the result can be written in the general form

$$\phi(r,t) \propto Q(r,t)/r, \tag{11}$$

where $Q(r,t)$ is the charge *screening factor*[9]. This factor has a trivial boundary condition $Q(0,t) \equiv 1$. According the Debye-Hückel theory[1], in equilibrium $Q(r) = \exp(-\kappa r)$, where κ is an inverse of the Debye length, $r_D = \kappa^{-1}$. Since we consider the non-equilibrium case, the charge screening can differ significantly from that in the equilibrium, in particular it could be time-dependent. Moreover, as shown in Ref.[9], for systems with charges or diffusion asymmetry each type of charges is screened differently. In general, it is necessary to use two factors, $Q_A(r,t)$ and $Q_B(r,t)$, for each type of particles.

4 Results

4.1 System without Coulomb interaction

We begin presentation of the results with an important limiting case of the system without electrostatic interaction when parameter $\zeta \equiv 0$. In this system particles of one kind, say A, attract each other, thus creating aggregates. At the same time, they repel from the particles of another kind B. This is a system with the similar-particle aggregation and segregation of dissimilar particles (phase separation)[10]. In this case, the basic physical mechanism that determines the kinetics of the process is the Ostwald ripening[31]: small NPs aggregates are absorbed by larger aggregates. The kinetics of this process is very slow, asymptotically it could end up with the survival of a single super-aggregate. For temperatures selected in this section rather loose super-aggregates occur, with the typical structure of a dense fluid.

As can be seen from Fig.2a, the oscillatory behavior of the joint correlation functions for similar particles, $F_{\alpha\alpha}(r,t)$, points to the formation of short-range (or intermediate) order typical for liquid. The degree of the ordering changes with time, which is natural for the formation of dense aggregates. With increasing temperature (parameter θ), short-range order is weakening, the oscillation amplitude of the correlation functions decreases. At the same time, when the temperature de-

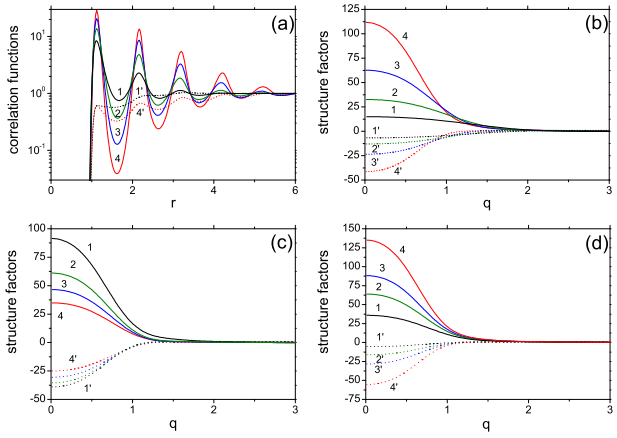

Fig. 2 (Color online) Binary system without Coulomb interactions, $\zeta = 0.0$, at intermediate temperatures. (a) The joint correlation functions $F_{\alpha\beta}(r,t)$ (solid line - similar, dot line - dissimilar, numbering with prime). Parameters: $[\eta, \theta, \mu = 0.4, 0.5, 0.5]$. Curves are shown for times t: (1) 2^{14}, (2) 2^{16}, (3) 2^{18}, (4) 2^{20}. (b) The structure factors $S_{\alpha\beta}(q,t)$ (solid line - for similar and dot line - for dissimilar pairs) for the same time t. (c) The structure factors at time $t = 2^{20}$ for the fixed density, $\eta = 0.4$, and different temperatures θ: (1) 0.6, (2) 0.8, (3) 0.9, (4) 1.0. (d) The structure factors at time $t = 2^{20}$ for the fixed temperature, $\theta = 0.5$, but different densities η: (1) 0.1, (2) 0.2, (3) 0.3, (4) 0.5.

creases, this type of order becomes more noticeable (crystallization). The behavior of the joint correlation functions for dissimilar particles, $F_{AB}(r,t)$, is more trivial and does not indicate the existence of any order (only noticeable effect of the excluded volume on a small length scale).

Note that we show here the results for the long simulation times $t = 2^m$ (in units of t_0), where the maximum value of the index $m = 24$ (this corresponds to the time $t \sim 10^7$). The small value of the base (two) was chosen using the following considerations: except generally slow changes of the structure, in certain parameter areas relatively fast restructuring was detected. To understand the range of times calculated in this paper, we note that the best result for 3d systems without electrostatic interaction achieved in the Ref.[32] (KMC) is only $t \sim 10^3$. In the case of the polar media absence studied here, where formally each particle interacts with all the others, the KMC time limit becomes $t \sim 10^1$. In this case, even a single particle can move only a short distance, of the order of the NP diameter, r_0, so that particles do not have enought time to build the structure. At the same time, in our simulations the diffusion of free particles occurs on time scale $t \sim 10^7$ or the distance $\sim 10^3 r_0$ which allows us reliable simulations of DySA.

More appropriate, however, to analyze the SA structures not in terms of short-range ordering, but from the point of view of the possible large-scale fluctuations in the system. Here, the fundamental characteristic of the system are structure factors $S_{\alpha\beta}(q,t)$, eq.(10). As can be seen from Fig.2b, at at fixed temperature, but different times, the similar patterns occur. The structure factors $S_{\alpha\alpha}(q,t)$ for the similar particles have a maximum, the amplitude and half-width of the peaks systematically increase with time (aggregation). At the same time, the structure factor $S_{AB}(q,t)$ for dissimilar particles has a minimum in the same range of q (particle segregation). Moreover, as can be seen from Fig.2c and Fig.2d, the same behavior is observed also by varying temperature (at fixed density) and by varying density (at fixed temperature). In other words, changing the parameters of the system (θ and η) changes only the kinetic parameters (rate of of structure formation), but the type of structure remains *universal*.

The structure in Fig.2 has a known counterpart - the equilibrium statistical system near the *critical point*, which is traditionally described by the Ornstein-Zernike theory[33,34]. It is known that near the critical point long-wavelength ($q \to 0$) fluctuations of particle density are developed. These density fluctuations show the emergence of correlation - particle aggregates. In the above-described system we studied the Ostwald ripening – the mechanism which also leads to the appearance of aggregates, which, unlike the physics of equilibrium phenomena, are not stationary. There the long-wavelength part of the fluctuation spectrum is not stable. As time increases, the system evolves to a critical point, which corresponds to an infinitely large time, $t \to \infty$. Note that the non-equilibrium critical phenomenon is not completely identical to its equilibrium counterpart. The non-linear fit for factors $S_{\alpha\alpha}(q,t)$ shows that their behavior corresponds to the Lorentz curve, $S(q_c)/[1+\xi^2(q-q_c)^2]$ with time-dependent small parameter q_c. In contrast, in the equilibrium case ξ is the correlation length and the parameter $q_c \equiv 0$[33,34].

Another analog of this behavior could be found in the structural characteristics of the bimolecular chemical processes[24,35]. The effects of segregation and aggregation there, however, are not caused by the interaction of particles, which we study here, but by chemical reactions. Moreover, it was shown that chemical reactions for systems with short-range interactions lead to non-equilibrium critical phenomena that, in turn, form long-range correlations. In the case of chemical reactions, the non-trivial critical exponents (depending on the space dimension) can be determined, i.e. use the terminology of critical phenomena is justified here. It was demonstrated by a comparison of a large number of examples with results of Monte Carlo simulations, that our theoretical method leads to the exact values of nontrivial critical exponents describing bimolecular diffusion-controlled kinetics[24,35].

The structure formation rate increases with decreasing tem-

perature and increasing particle density. Therefore, in the study of structures of a certain type, we prefer to show results for dense systems, for which the direction of the process is more clear. It should be noted that the studied systems are characterized by large characteristic relaxation times, so the results for short times can differ considerably from those for the long time.

This analysis can be extended by using RMC method[28]. Fig.3 shows the characteristic snapshots for a set of parameters

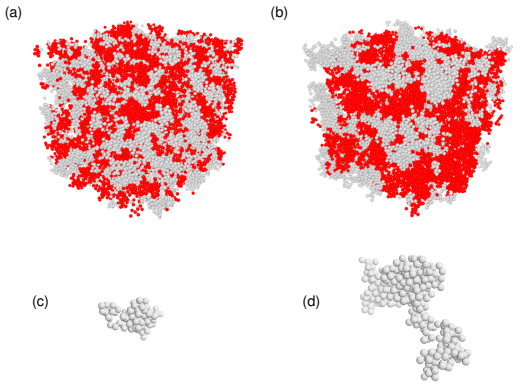

Fig. 3 (Color online) Characteristic 3d structure snapshots obtained using the RMC: (a,b) corresponds to the structure factors for $[\eta,\theta,\mu=0.2,0.7,0.5]$ and the times (a) 2^{20} and (b) 2^{24}, whereas (c,d) show the maximal domain for snapshots (a,b).

$[\eta,\theta=0.2,0.7]$. Transient structures are detected in Fig.3a,b. For all times aggregates are homogeneous in their composition (domains with one type of particles), Fig.3c,d. Here, for each case a maximum size of one domain is shown. At long times, the domains do not have a spherical shape, Fig.3d, due to a inpenetration of the different types of domains, the structure becomes a labyrinth type.

Incorporation of the electrostatics into the system is characterized by the parameter ζ. Depending on its value, different types of structures could arise. Let us conditionally classify the range of values $\zeta<\zeta_0\sim 1$ as a weak Coulomb interaction, and $\zeta\gg\zeta_0$ a strong Coulomb interaction.

4.2 Weak Coulomb interaction

Incorporation of the electrostatic interaction leads to new effects as compared with the Section 4.1. Since the mutual attraction of similar particles at short distances is stronger than their Coulomb repulsion, similar particles retain a trend to form dense aggregates (domains). However, unlike the previous case, the domains cannot indefinitely increase in size due to the effect of Ostwald ripening. Coulomb repulsion of the similar particles within the domain makes it unstable. A linear domain size λ is a function of the parameters θ and ζ. At distances exceeding λ the short-range interactions could be neglected. Here, the only effect is the Coulomb interaction between domains, and it is strong. The fact that each domain contains a large number of similar particles N means that at distances $r\gg\lambda$ it acts as a super-particle with a big charge, Ne. Ionic crystallization occurs between domains of opposite charges, the result is the structure with the characteristic charge oscillations.

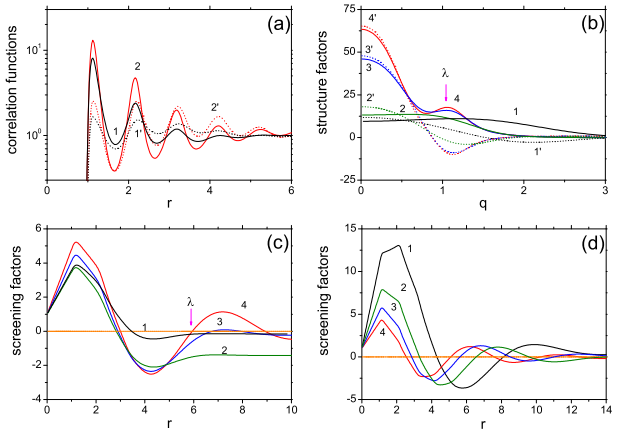

Fig. 4 (Color online) Windows (a-c): Ionic binary systems with Lennard-Jones and Coulomb interactions for fixed parameters $[\eta,\theta,\mu,\zeta=0.4,0.5,0.5,0.5]$. Solid line - similar and dot line - dissimilar pairs (numbering with prime). (a) shows the joint correlation functions for times t: (1) 2^{18}, (2) 2^{24}. (b) - the structure factors for the times t: (1) 2^{17}, (2) 2^{18}, (3) 2^{20}, (4) 2^{24}. (c) shows the screening factors $Q(r,t)=Q_A(r,t)=Q_B(r,t)$ for the same times as in (b). The window (d) shows the screening factors $Q(r,t)$ at time $t=2^{24}$ for the fixed temperature, $\theta=0.4$, but different values of parameter ζ: (1) 0.25, (2) 0.50, (3) 0.75, (4) 1.00.

Fig.4 shows that in the modeled time range the simulated correlation functions are not stationary, the process of structure formation continues. The behavior of the structure factors, Fig.4b, indicates the occurrence of a fundamentally new type of structure without particle segregation. At long times, *all the structure factors* reveal maxima with close magnitudes. The non-linear fit of the Lorentz type, $S(q_c)/[1+\xi^2(q-q_c)^2]$, occurs for all factors $S_{\alpha\beta}(q,t)$. We can see systematic increase with time of the peak maxima at $q=0$ and their half-widths. In other words, this is a non-equilibrium critical phenomenon, studied previously in a simple form in the Section 4.1, where the large-scale density fluctuations occur. However, aggregates are not composed of particles of one type, they are made now of domains with different charges.

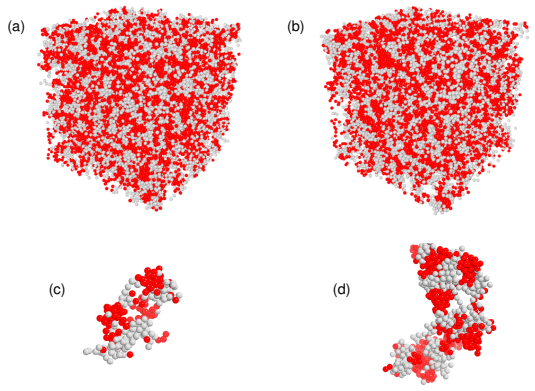

Fig. 5 (Color online) Same as Fig.3 for parameters $[\eta, \theta, \zeta = 0.2, 0.6, 0.4]$ and the times (a) 2^{20} and (b) 2^{22}.

The above-said becomes more clear when looking at the characteristic 3d snapshots, Fig.5. It is seen that with increasing time the size of the aggregates also increases. The aggregates are not homogeneous, they have a complex heterogeneous structure (composed of homogeneous domains). These results are qualitatively agree with those in Refs.[6,7,9,10] for two-dimensional systems. As one can see, the competition of weak electrostatic and short-range interactions leads to formation of the structures with oscillating charges. Parameters of the resulting structure can be estimated in different ways. One can see in Fig.4b the emergence of additional extremes at $q = q_0 \approx 1$: the local maximum for similar structure factors and the local minimum in the same area for dissimilar structure factors. This extremum is formed only at very long times, curves (3,4), and then does not change with time. This value may be associated with the previously mentioned characteristic length $\lambda = 2\pi/q_0$ (the size of the domain or the oscillation period of the charge). Since the value $q_0 \sim 1$, one can estimate $\lambda \approx 6$ (in units r_0), which is consistent with results in Fig.5c,d.

The above-said is confirmed by the analysis of Fig.4c, where the behavior of the screening factors, eq.(11), is shown for the same time range. At short times a quasi-equilibrium charge distribution is not established yet, so the Coulomb interaction of NPs is not fully screened, $\lim_{r\to\infty} Q(r,t) \neq 0$, see curves (1,2). As time increases, the Coulomb interaction becomes screened, $\lim_{r\to\infty} Q(r,t) \approx 0$. This result is in a qualitative agreement with the Debye-Hückel theory. However, the overall behavior of the screening factors is very different from the predictions of the standard Debye-Hückel theory[1,9]: they show oscillations. This result is not surprising. In the Debye-Hückel theory, in a well stirred system each charge is supposed to be surrounded by a cloud of particles with opposite charges. In our case, a very different structure is formed: a given particle is surrounded by a cloud of *similar* particles forming a homogeneous domain. At the distances $\sim \lambda$ it sticks to a domain with an opposite charge. This results in the characteristic structure with oscillating charges, Fig.5c,d. As follows from the behavior of the curve (4) in Fig.4c, the oscillation period of the charge is of the order $\lambda \approx 6$, which is consistent with the previous estimate.

The consistency of the results are not surprising, since as shown in the Section 3.3, all the fundamental system characteristics are obtained from the same correlation functions by the transformation of the information (Fourier transform, eq.(10), the mapping of information from correlation functions into the characteristic snapshots, or solving directly the Poisson eq.(7)).

Snapshots Fig.5c,d allow us to anticipate the structure of the studied system at long times, i.e. in fact in equilibrium. It is a quasi-periodic (as far as it is possible for a dense fluid) structure with the charge oscillations. Qualitatively, it does not differ from that previously discussed in Ref.[6] for a special case of two-dimensional system.

Additionally, Fig.4d shows the behavior of the screening factors at fixed time, but for different values of the parameter ζ. The systematic increase of this parameter results in decrease of both the amplitude of the oscillations in the screening factors and the oscillation period λ. With further increase of the parameter ζ the aggregate growth stops, the system is quickly relaxed to the stationary (equilibrium) structure. Thus, suggested definition of the weak Coulomb interaction, $\zeta < \zeta_0 \sim 1$, is justified by the results of kinetics. In other words, for $\zeta = \zeta_0$ the *kinetic phase transition* is observed between the two kinetic regimes: stationary and non-stationary ones (non-equilibrium critical phenomenon).

4.3 Diffusion asymmetry

As could be seen from the kinetic eqs.(6), the partial diffusion coefficients D_α directly control the process kinetics. Therefore, in general, the asymmetry in the NP mobilities has to produce asymmetry in other characteristics, in particular the structure, or the screening factors. This statement is not, however, universal. The equilibrium state is described by the stationary solution of the eqs.(6) which does not depend on the kinetic characteristics - diffusion coefficients. That is, the equilibrium restores symmetry between particles. Therefore, the asymmetry is particularly noticeable only at relatively short times, when the structure of the system is far from equilibrium. In the regime of a slow change in the structure the quasi-equilibrium situation occurs.

These general statements are confirmed by Fig.6. As one can see in Fig.6a, the asymmetry of the correlation functions is obvious at short times, where $F_{AA}(r,t) \neq F_{BB}(r,t)$. However,

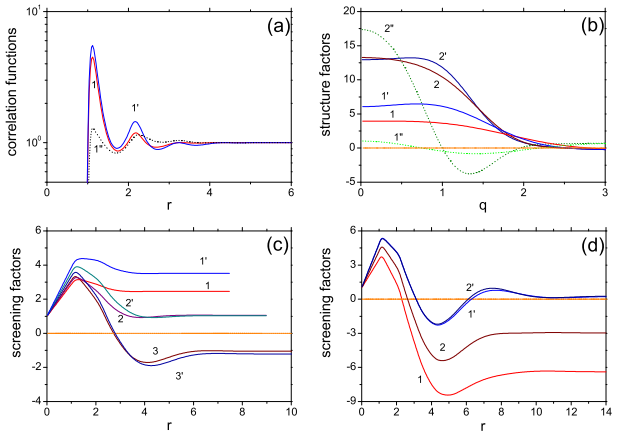

Fig. 6 (Color online) Windows (a-c): Ionic binary systems with both Lennard-Jones (short-range) and Coulomb (long-range) interactions and asymmetric diffusion. Parameters: $[\eta,\theta,\mu,\zeta=0.4,0.5,0.2,0.5]$. Solid line corresponds to similar- whereas dot line - dissimilar NP pairs. (a) the joint correlation functions for the times $t=2^{14}$ (curve (1) AA, curve $(1')$ BB, and $(1'')$ AB correlations). (b) the structure factors for the times t: (1) 2^{12}, (2) 2^{14}. (c) the screening factors $Q_A(r,t)$ (curves without primes) and $Q_B(r,t)$ (curves with primes) for the times (1) 2^{14}, (2) 2^{16} and (3) 2^{18}. The window (d) shows the screening factors at time $t=2^{22}$ for the same parameters $[\eta,\theta,\zeta=0.4,0.5,0.5]$, but two different values of mobility μ: (1) 0.05 and (2) 0.10.

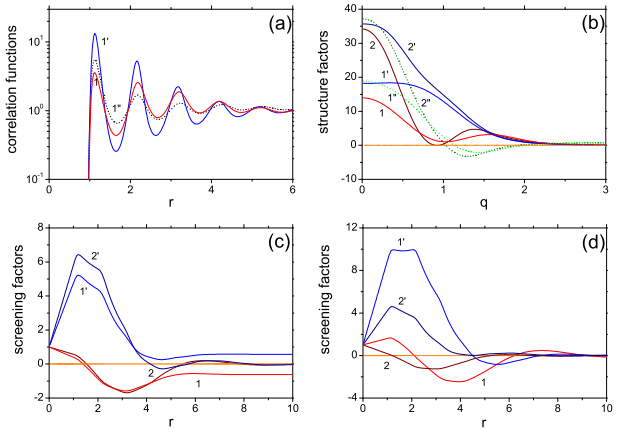

Fig. 7 (Color online) (a-c) Ionic binary systems with Lennard-Jones and Coulomb interactions for asymmetric particle charges, $Z_A=2, Z_B=1$. Parameters: $[\eta,\theta,\mu,\zeta=0.4,0.5,0.5,0.5]$. Solid line - for similar and dot line - for dissimilar pars. (a) shows the joint correlation functions for the time $t=2^{24}$ (curve (1) AA, curve $(1')$ BB, and $(1'')$ AB correlations). (b) the structure factors for the times t: (1) 2^{18}, (2) 2^{24}. (c) the screening factors $Q_A(r,t)$ (curves without primes) and $Q_B(r,t)$ (curves with primes) for the same times. (d) shows the screening factors at times $t=2^{24}$ for the same parameters $[\eta,\theta,\mu=0.4,0.5,0.5]$, but with two different values of ζ: (1) 0.25 and (2) 0.75.

the transition to a quasi-stationary regime occurs very fast, see Fig.6b for the structure factors. Even at times $t=2^{14}$ the difference between factors becomes negligible. The same applies to the screening actors, Fig.6b. Retention time to the quasi-stationary regime strongly depends, however, on the degree of asymmetry in the particle mobilities. It is relatively small, $\mu=0.2$, in the case shown in Figs.6a,b,c. For a comparison, Fig.6d shows examples of a very strong diffusion asymmetry, $\mu=0.05$ and $\mu=0.10$, that leads to asymmetry of basic characteristics at much longer times. Since in this paper we are primarily interested in the long-time behavior of the kinetic characteristics, we restrict ourselves to cases of symmetric diffusion.

4.4 Asymmetry of particle charges

Another, more significant asymmetry parameter is the difference of particle charges. Here, the symmetry between particles could never be restored. Fig.7 shows the results for the system, where the charge of one type of particles twice exceeds that of other particles: $Z_A=2$ and $Z_B=1$. Accordingly, for the electrical neutrality we assume $n_B/n_A=2$. The correlation functions $F_{AA}(r,t)\neq F_{BB}(r,t)$, Fig.7a, the structure factors $S_{AA}(q,t)\neq S_{BB}(q,t)$, Fig.7b, or the screening factors $Q_A(r,t)\neq Q_B(r,t)$, Fig.7c, are always different. It is easy to understand the reason for this: particles with a larger charge, A, are isolated from each other. They are mainly surrounded by a cloud consisting of a large number of another-type particles, B (with a smaller and opposite charge). Therefore, the *effective* charge of the particle A decreases rapidly with the increasing distance, and moreover, even changes its sign. At the same time, the particles B, which are in excess, aggregate into domains. Their effective charge, determined by a number of similar particles in the domain, can turn out to be quite large. Thus, in Fig.7c the effective charge of the particle within the domain is ~ 6. Outside the boundary of the similar-particle domain a cloud of particles of opposite charge occurs, so that the effective charge with the distance from domain begins to behave asymptotically in the spirit of Debye-Hückel theory: the screening factor tends to zero. Fig.7d shows the behavior of the structure factors for different values of parameter ζ. As one can see, varying the parameters, the nature of the screening charges can change strongly, and has nothing to do with the results of the standard Debye-Hückel theory.

The above statement could be illustrated quite clearly by the characteristic snapshots in Fig.8. Despite the fact that the *full-*

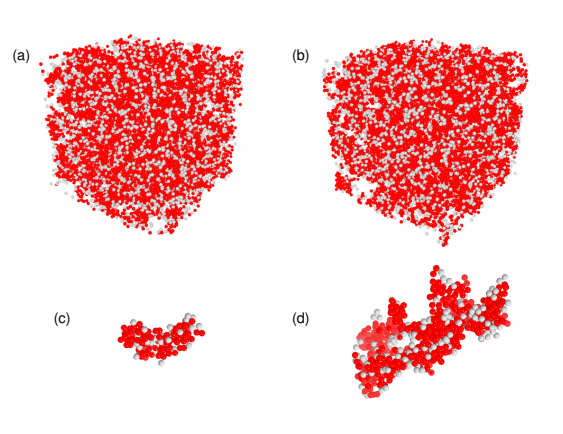

Fig. 8 (Color online) Characteristic 3d structure snapshots obtained using the RMC. They correspond to the correlation functions for $[\eta, \theta, \mu, \zeta = 0.2, 0.6, 0.5, 0.5]$, times: (a) 2^{20} and (b) 2^{24}.

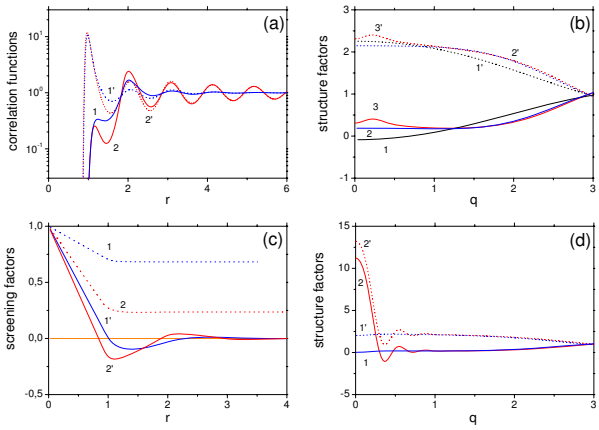

Fig. 9 (Color online) (a-c) Ionic binary systems with Lennard-Jones and Coulomb interactions for fixed parameters $[\eta, \theta, \mu = 0.1, 1.0, 0.5]$ (small density and strong Coulomb interaction). Solid line - for similar and dot line - for dissimilar pairs. (a) the joint correlation functions for two values of parameter ζ: (1) 40.0 and (2) 50.0. (b) the structure factors for the times t: (1) 2^8, (2) 2^{12}, (3) 2^{24}. Parameter $\zeta = 50.0$. (c) the screening factors $Q_A(r,t) = Q_B(r,t)$ for the time $t = 2^6$ (1,2) and $t = 2^{24}$ $(1', 2')$ and two values of parameter ζ: $(1, 1')$ 20.0 and $(2, 2')$ 60.0. The window (d) shows the structure factors at time $t = 2^{24}$ for two values of parameter ζ: (1) 45.0 and (2) 55.0.

size snapshots, Fig.8a,b, visually differ only slightly, the analysis of the behavior of *maximal-size* clusters, Fig.8c,d, shows that the non-equilibrium critical phenomenon also takes place here: the size of aggregates slowly but continuously increases with time.

4.5 Strong Coulomb interaction

As already noted, an increase of parameter $\zeta > \zeta_0 \sim 1$ characterizes the contribution of the electrostatic interaction leads to disappearance of the non-equilibrium critical phenomenon: the solutions of kinetic equations quickly converge to the asymptotic equilibrium behavior. In this case, the correlation functions differ from their asymptotic values, eq.(9), only at the very short distances $\sim r_0$. In other words, in this kinetic mode only small clusters are formed, whose further aggregation into large clusters is not possible. Structure of the system in equilibrium corresponds to the real gas, however, where the structural elements are not individual nanoparticles, but small neutral clusters built from nanoparticles. In the case of a weak Coulomb interaction (Section 4.2), small changes of the parameter ζ have led to strong changes of all the results, whereas in this kinetic mode, the results are much less sensitive to the values of the parameter ζ.

However, for very large values of the parameter $\zeta > \zeta_c$, the *second* kinetic phase transition takes place. Here, small clusters begin to connect to large ones resulting in ionic *crystallization*. For such large values of ζ, the contribution of short-range attraction becomes unimportant. Therefore, only the effect of excluded volume occurs and the results practically do not depend on the parameter θ. In Fig.9 we have chosen its relatively large value, $\theta = 1$.

Fig.9a shows the behavior of the correlation functions for long times, $t = 2^{24}$, and the two large values of ζ. The value of $\zeta = 40$ corresponds to the steady-state (equilibrium). The characteristic snapshots differ only slightly from those shown in Fig.10, because the results change very little with increasing the parameter ζ, until the second critical point, $\zeta = \zeta_c$, arises. However, with an increase of ζ up to $\zeta = 50$, the behavior of the correlation functions changes quite dramatically: non-equilibrium ordered structures are created where the aggregate size is continuously growing. In other words, ionic crystals start to grow in this parameter area. Note that these results can be compared to Refs.[18,19], where, however, the electrostatic interaction was taken in the limit of high salt concentrations (the long-range Coulomb potential was replaced by the short-range Yukawa potential).

Fig.9b shows the behavior of the structural factors for the same values $\zeta = 50$. First, we note that the amplitudes of all the factors are extremely small, unlike the cases discussed in the previous sections. This corresponds to the fact that there are no longer large aggregates in the system. However, it can be seen that for a very long time $t = 2^{24}$ an anomaly in the behavior of the factors near $q = 0$ occurs. Exploring other parameter values ζ, Fig.9d, assures that the critical value ζ_c is close to $\zeta_c \approx 50$. For $\zeta < \zeta_0$ the structure factors are station-

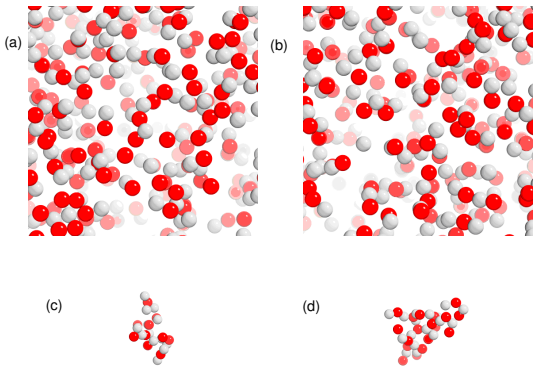

Fig. 10 (Color online) Characteristic 3d structure snapshots obtained using the RMC: (a,b) corresponds to the correlation functions for $[\eta, \theta, \mu = 0.1, 1.0, 0.5]$ and ζ: (a) 20 and (b) 45, whereas (c,d) shows the maximal clusters for snapshots (a,b). The times $t = 2^{24}$

ary and small. In contrast, as $\zeta > \zeta_c$, they are not stationary and show a peak near $q = 0$. Thus, Fig.9b corresponds to the critical point.

Although for the parameter $\zeta \sim \zeta_c$ the structure factors can greatly vary, the screening factors remain practically unchanged, Fig.9c. Moreover, they rapidly approach to the asymptotic values. The nature of the screening is almost independent on the kinetic mode (non-equilibrium critical phenomena, or equilibrium). In other words, the type of charge screening, observed earlier in the equilibrium for a system of small stable clusters, continues to occur in the mode of large aggregate growth. This becomes clear from the characteristic snapshots for maximum-size clusters, Fig.10c,d. The aggregates here are not dense systems, they form rather dendritic structures (of loose clusters). Such the structure formation could be explained by the strong Coulomb interactions between the particles. Since the particle binding becomes hard to break, any structural rearrangements (formation of a dense aggregates) become very complicated.

5 Conclusions

In this paper, the electrostatic dynamic self-assembling was investigated for ionic three-dimensional systems. For the first time, the very important limiting case is studied in detail, in which the screening of the nanoparticles occurs only as the result of particle spatial rearrangement (without polar solvent screening long-range Coulomb interactions). The integrated approach (analytical and numerical solution of nonlinear self-consistent kinetic equations) was developed and applied. This approach allows us to investigate the kinetics of the process for very long time, which is impossible by means of traditional methods (Kinetic Monte Carlo or Molecular Dynamics). We obtained a complete set of statistical characteristics of the system, including the sets of the joint correlation functions (radial distribution functions), partial structure factors, as well as the charge screening factors. This fundamental information is accompanied with the characteristic snapshots obtained by 3d Reverse Monte Carlo method. It was shown that within a certain range of control parameters, a continuous growth of aggregates occurs, from small ones to big. The particle aggregates reveal a complex structure with the characteristic charge oscillations. The kinetics of the aggregation process was analyzed from the point of view of non-equilibrium physics of critical phenomena: we have established the existence of the large-scale critical fluctuations of the particle densities. It is also shown that in many systems with dynamical self-assembling, the screening of the particle charges could strongly differ from the standard Debye-Hückel theory for equilibrium systems. The results obtained could be important for understanding of the fundamental aspects of DySA in charged nanoparticle systems in chemistry, physics and biology.

Acknowledgments

VK thanks the the Non-Equilibrium Energy Research Center (NERC) which is an Energy Frontier Research Center funded by the U.S. Department of Energy, Office of Science, Office of Basic Energy Sciences under Award Number DE-SC0000989 for partial support. This work was partly supported by Latvian grant 237/2012. Authors are greatly indebted to M. Olvera de la Cruz for numerous fruitful discussions.

References

1 D. A. Walker, B. Kowalczyk, M. Olvera de la Cruz, and B. A. Grzybowski, *Nanoscale*, 2011, **3**, 1316.
2 E. V. Shevchenko, D. V. Talapin, N. A. Kotov, S. O'Brien, C. B. Murray, *Nature*, 2006, **439**, 55.
3 R. J. Macfarlane, B. Lee, M. R. Jones, N. Harris, G. C. Schatz, C. A. Mirkin, *Science*, 2011, **334**, 204.
4 B. A. Grzybowski, B. Kowalczyk, I. Lagzi, D. Wang, K. V. Tretiakov and D. A. Walker, *Faraday Discuss.*, 2012, **159**, 201.
5 *Self-Assembled Materials*, special issue of Polymer Journal, 2012, **44**, issue 6.
6 S.M. Loverde, F.J. Solis, and M. Olvera de la Cruz, *Phys. Rev. Lett.*, 2007, **98**, 237802.
7 S.M. Loverde, Y.S. Velichko, and M. Olvera de la Cruz, *J. Chem. Phys.*, 2006, **124**, 144702.
8 V.N. Kuzovkov, E.A. Kotomin, G. Zvejnieks, M. Olvera de la Cruz, *Phys. Rev. E*, 2010, **82**, 021602.
9 V.N. Kuzovkov, E.A. Kotomin, and M. Olvera de la Cruz, *J. Chem. Phys.*, 2011, **135**, 034702.

10 V.N. Kuzovkov, E.A. Kotomin, and G. Zvejnieks, *J. Phys. Chem. B*, 2011, **115**, 14626.

11 A. Warshel and S.T. Russell, *Quarterly Reviews of Biophysics*, 1984, **17**, 283.

12 A.G. Cherstvy, *Phys.Chem.Chem.Phys.*, 2011, **13**, 9942.

13 A. Gautam and F.C.J.M. van Veggel, *J. Mater. Chem. B*, 2013, **1**, 5186.

14 A. Walcarius, S.D. Minteer, J. Wang, Y. Lin, and A. Merkoci, *J. Mater. Chem. B*, 2013, **1**, 4878.

15 W.G. Noid, *J. Chem. Phys.*, 2013, **139**, 090901.

16 B.A.Grzybowski, H.A. Stone, G.M. Whitesides, *Nature*, 2000, **405**, 1033.

17 G.M. Whitesides and B.A. Grzybowski, *Science*, **295**, p.2418 (2002).

18 R. Orlik, A.C. Mitus, B. Kowalczyk, A.Z.Patashinski, and B.A. Grzybowski, *J. Non-cryst. solids*, 2009, **355**, 1360.

19 Rui Zhang, P.K. Jha, and M. Olvera de la Cruz, *Soft. Matter.*, 2013, **9**, 5042.

20 V.N. Kuzovkov, E.A. Kotomin, and G. Zvejnieks, *J. Chem. Phys.*, 2011, **135**, 224503.

21 Kokorin A (editor). *Ionic Liquids: Theory, Properties, New Approaches*; Croatia: InTech, 2011.

22 A. Naji, M. Kanduč, J. Forsman, and R. Podgornik, *J. Chem. Phys.*, 2013, **139**, 150901.

23 D. Frenkel and B. Smit, *Understanding Molecular Simulation*; Academic Press, 2001.

24 E. A. Kotomin and V. N. Kuzovkov, *Modern Aspects of Diffusion-Controlled Reactions: Cooperative Phenomena in Bimolecular Processes*, Vol. 34 of *Comprehensive Chemical Kinetics* (Elsevier, North Holland, Amsterdam, 1996).

25 E.A.Kotomin and V.N.Kuzovkov, *Rep. Prog. Phys.*, 1992, **55**, 2079.

26 J.G. Kirkwood, *J. Chem. Phys.*, 1935, **3**, 300.

27 T.E. Faber and J.M. Ziman, *Philos. Mag.*, 1965, **11**, 153.

28 G. Zvejnieks, V.N. Kuzovkov, and E.A. Kotomin, *Phys. Stat. Sol. (a)*, 2014, **211**, 288.

29 R.L. McGreevy and L. Pusztai, *Mol. Sim.*, 1988, **1**, 359.

30 R.L. McGreevy, *J. Phys.: Condens. Matter*, 2001, **13**, R877.

31 R. Boistelle, J.P. Astier, *J. Cryst. Growth*, 1988, **90**, 14.

32 P. K. Jha, V. Kuzovkov, B. A. Grzybowski, M. Olvera de la Cruz, *Soft Matter*, 2012, **8**, 227.

33 L.S. Ornstein and F. Zernike, *Proc. Acad. Sci.*, Amsterdam, 1914, **17**, 793.

34 H.E. Stanley, *Introduction to phase transitions and critical phenomena* (Oxford Univ. Press, Oxford, 1971).

35 V.N.Kuzovkov and E.A.Kotomin, *Rep. Prog. Phys.*, 1988, **51**, 1479.